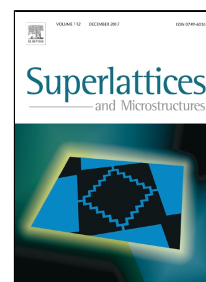# Accepted Manuscript

Artificial Neural Network modeling and sensitivity analysis for soiling effects on photovoltaic panels in Morocco

B. Laarabi, O. May Tzuc, D. Dahlioui, A. Bassam, M. Flota-Bañuelos, A. Barhdadi

Please cite this article as: B. Laarabi, O. May Tzuc, D. Dahlioui, A. Bassam, M. Flota-Bañuelos, A. Barhdadi, Artificial Neural Network modeling and sensitivity analysis for soiling effects on photovoltaic panels in Morocco, *Superlattices and Microstructures* (2017), doi: 10.1016/j.spmi. 2017.12.037

Artificial Neural Network modeling and sensitivity analysis for soiling effects on photovoltaic panels in Morocco

B. Laarabi[1], O. May Tzuc[2], D. Dahlioui[1], A. Bassam[2*], M. Flota-Bañuelos[2], A. Barhdadi[1*]

[1]Semiconductors Physics and Solar Energy Research Team (PSES)
Energy Research Centre, Ecole Normale Supérieure (ENS)
Mohammed V University in Rabat, Morocco

[2]Faculty of Engineering, Autonomous University of Yucatan,
Av. Industrias no contaminantes, Merida, Yucatan, Mexico

Abstract

In the present work, an Artificial Neural Network (ANN) methodology for studying and modeling the soiling effect on solar photovoltaic (PV) glass is presented. To perform the study, a solar PV glazing was exposed outdoor at the home solar energy platform of Physic of Semi-conductors and Solar Energy research structure (PSES) at Mohammed V University in Rabat, Morocco. Regular measurements from April 20, to December 31, 2016, were carried out to monitor the soiling rate changes over time. Meteorological data were used as input variables for ANN modeling. The model performance was evaluated using a statistical comparison between experimental and simulated values. Results show that the implementation of Levenberg-Marquardt backpropagation algorithm, and the active functions Tansig, and Purline achieve the best estimations ($R^2 = 0.928$) in an ANN architecture 6-35-1. Additionally, a sensitivity analysis approach was employed to determine the effect of input parameters on model output and the behavior of the model with the variation of each input parameter. Sensitivity analysis results indicate that the most influential parameter for PV soiling rate was the relative humidity, followed by wind direction. The ANN model coupled with sensitivity analysis show be a promising framework for its application in smart sensors on cleaning systems for PV modules to improve their operational efficiency.

Keywords: Solar energy; soiling effect; solar PV glass; ANN application; PAWN sensitivity analysis.

36   *Corresponding author

37   *Email address*: abarhdadi@yahoo.fr (A. Barhdadi)

38   *Email address*: baali@correo.uady.mx (A. Bassam)

39

41

42

43

44

45

46

47

48

49

50

51

52

53

54

55

56

57

58

59

60

61

62

63

1. INTRODUCTION

Morocco is considered the largest potential markets for renewable energies in the region of Meddle East and North Africa (MENA), thanks to excellent solar resources throughout the country and wind resources along Atlantic Coast [1]. The potential of solar energy in Morocco is estimated at 3000 hours/year, hence the launch of the Moroccan Solar Plan to reach 2 Gigawatts by 2020. Unfortunately, the sites where the solar energy is important, characterized, in most cases, by harsh weather conditions which can increase the probability of material degradation and also provoke severe dust accumulation [2]. This last parameter is named soiling or dusting and it is mostly a mixture of small amounts of organic particles and/or minerals from geomorphic fallout such as sand, clay, or eroded limestone.

In Morocco, just a few studies have been conducted in order to study the effect of this phenomenon on the performances of PV (Photovoltaic)/CSP (Concentrated Solar Power) modules and systems. Table 1 presents a summary of the studies performed in Morocco, their locations as well as their results. From this, it can be clearly seen that six studies have been conducted in eight Moroccan cities belonging to semi-arid, arid, and extremely arid climates. They all proving the relevance of the topic considered in this work. The studies include the losses during the exposure period, the effect of tilt angle, the determination of factors affecting soiling, and modeling of this phenomenon using time series. It can also be seen that modeling of soiling phenomenon in Morocco still need more studies, which prove that each addition in that subject will be of such importance.

Table 1. Studies of soiling effect on PV/CSP modules conducted in Morocco

Category	Technology	Region	Results	Ref
Investigation	CSP	Skoura (40 km from Ouarzazat)	The soiling rate is a function of the variation of the wind speed and the relative humidity during the exposure.	[3]
	CSP	Oujda	The drop in cleanliness is: - 45% and 33% for glass and mirrors in aluminum, respectively in a horizontal position. - 14% for both reflectors at an angle of +45°. For mirrors installed at 0° and -45° angles remained clean with a purity average of about 97% for both types of mirrors.	[4]
	PV-modules irradiation sensors	Atlantic Ocean	The efficiencies dropped to 20% of the initial values within 5 months.	[5]
	CdTe PV	Marrakech, Ouarzazate,	Estimates of the change in average monthly CdTe PV performance due to soiling are 0 to <-3% with cleaning.	[6]

3

		Oujda, Dakhla		
	PV/HCPV (High Concentration Photovoltaics)	Rabat	Transmittance losses of a solar PV glass due to soiling are approximately 5% per three months. Productivity losses of HCPV modules are approximately 7,64% per one month.	[7] [8]
Modelling	CSP	Tantan, Agadir	The analysis of the cleanliness of a solar reflectors exposed outdoors has been performed using the free R software for statistical computing and graphics. The results have shown that the best-fitted model describing the long-term change in the cleanliness is the local linear trend, which performs even better when an optimal discount factor of 0.95 is considered.	[9] [2]

86

Soiling is depending on several parameters which have a double effect in most cases. These parameters can be gathered into five different groups: the nature of the surface, the weather conditions, the soiling properties, the exposure conditions, and the environmental conditions. Table 2 summarizes the various parameters as well as their effects on soiling. In this table we have tried to describe for each condition (higher, lower, big, small…) of each factor (wind speed, rainfall, tilt angle…) the nature of its effect, positive (+) or negative (-). We have also described the arguments behind this nature based on studies published in literature.

The content of this table shows the complexity of the soiling phenomenon because of depending on several environmental parameters at the same time. It is also proving that extensive investigations should be conducted with the objective to understand well this phenomenon.

The parameters mentioned in this table could be divided into two categories, static parameters and temporal parameters. The static parameters depend on recommendations of standards (nature of the surface, tilt angle), physical laws such as gravity (location) or the existing specifications of the chosen site (soil texture). The temporal parameters comprise weather conditions and soiling properties and they changed through time and differ from a season to another. Concerning the tracking it is a parameter that change through the day and from a season to another but it can be considered as static from a year to another. For birds dropping, it's a complex parameter that is difficult to predict. From this we can conclude that the weather conditions and soiling properties are the most relevant parameters affecting this phenomenon. Based on this conclusion we have tried to predict the effect of soiling from some weather conditions factors. Some of them, have been chosen from Table 1 and other

110 ones have been added in order to study their effect. The soiling properties and other

111 parameters will be included in the future improved model.

112

113 Table 2. Summary of the different parameters that could impact the soiling of PV modules.

Nature of the effect	Parameters	Conditions	Effect	Arguments	Ref
Nature of the surface	Nature of the surface	Low surface energy. Chemically neutral, smooth and hydrophobic surface.	+	Reduction of the adhesion forces of particles to the surface.	[10] [11]
Weather conditions	Wind speed	higher	+	Removal of dust from the surface.	[12] [13]
			-	The increase of aerosols in the air.	
	Moisture	Higher	+	Increased interparticle forces of soil particles, therefore, the need for high speeds for their transport.	[10] [11]
			-	The increase of interparticle forces of the particles deposited on the surface of the module, therefore, the need for high speeds for their transport.	
	Dew		-	Promoting cementing and adhesion of particles.	[14] [15]
	Rainfall	Heavy	+	Cleaning modules.	
		Low	-	Promoting cementing and adhesion of particles.	
Soiling properties	Particle Size	Small	- (Compared to big particles)	Shading of all the module surface	[13]
		Big	+ (Compared to small particles)	Shading of part of the module surface.	
	Composition	Opaque	-	Decrease the transmitted irradiance.	[11] [12]
		Translucent Transparent	+	Increase the transmitted irradiance.	
Exposure conditions	Tilt angle	Large	+	Removal of dust due to gravity.	[16]
		Low	-	Significant accumulation of dirt.	
	Location	Top	+	Less dust accumulation.	[16]
		Low	-	Large dust accumulation.	
	Tracking	With	+	Less dust accumulation.	[16]
		Without	-	Large dust accumulation.	
Environmental conditions	Bird droppings	In off-shore sites	-	Shading cells and creating hot spots.	[16]
	Soil texture	Compacted	+	Low concentration of aerosols in the air.	[12]
		Loose with sand	-	The increase of aerosols in the air.	

114

115 It is extremely difficult to study experimentally the PV panel losses due to soiling

116 everywhere, and there is an urgent need to model this phenomenon using appropriate

117 innovative approaches. Indeed, many countries are giving a high priority to developing

5

118 accurate soiling loss modeling and forecast soiling effect over time. In the last years,

119 Artificial Neural Networks (ANN) have been employed as a suitable tool for modeling

120 phenomena in PV systems, due to their robustness, noise tolerance and their ability to work

121 with multivariable and non-linear information. These techniques have been successfully

122 applied on PV systems for various purposes such as model the performance and the daily PV

123 energy power production [17,18]; temperature estimation for PV modules and PV arrays

124 [19,20]; modeling of characteristic curves for the development of new PV semiconductor

125 materials [21,22]; and implementation in Maximum Power Point Tracking (MPPT) PV

126 systems [23], to mention a few. In all these works, ANNs have been described as a suitable

127 tool for modeling different phenomena occurring in PV systems.

128 The aim of this work is to present an ANN methodology for modeling the soiling effect

129 on solar PV glass based on meteorological parameters. Additionally, a new sensitivity

130 analysis approach is proposed in order to determine the relative importance of the

131 meteorological parameters on the PV glass soiling effect. The paper is organized in the

132 following way. The next section constrains the experimental set-up description, the artificial

133 neural network theory, and the sensitivity analysis technique explanation. The third section

134 presents the results and discussions of ANN modeling and sensitivity analysis influence.

135 Finally, in the last section, the conclusions are pointed out.

136

2. MATERIAL AND METHODS

138 *2.1. Description of experimental design*

139 To perform the study, a solar PV glazing (Figure 1(a)) was exposed outdoor at home Solar

140 Energy Platform in Rabat. Regular measurements from April 20 to December 31, 2016, were

141 performed to monitor the change of soiling rate over time.

142 In this work, the effect of meteorological parameters (global solar irradiance, wind

143 velocity, wind direction, ambient temperature, relative humidity, and rainfall) on the soiling

144 rate of solar PV glass has been studied. Meteorological data have been recorded both from

145 the weather station (Figure 1(b)) installed in the Solar Energy Platform and from the

146 Moroccan Meteorology Department.

6

Figure 1. a) The solar PV glass installed in the outdoor conditions of Rabat-Morocco. b) The meteorological station installed in the solar energy platform of PSES, ENS-UM5-Rabat.

The soiling rate has been calculated using the following equations:

$$??_e = \frac{G - G_{moy}}{G} \tag{1}$$

$$G_{moy} = \frac{\sum\limits_{i=1}^{i=24} G_i}{24} \tag{2}$$

G and G_{moy} are respectively the received and the transmitted irradiance by the solar PV glass. The average transmitted irradiance was calculated by performing various spot irradiance measurements. The experimental procedure is as follows:

1. The standard solar PV glass used in our experiment is supposed divided into 24 elementary rectangles of equal dimensions (27.5 cm x 24.5 cm).

2. For each elementary rectangle, the received irradiance G and the transmitted one G_i are regularly measured every day at noon, using a solar power meter placed at the center of both sides of the rectangle. This operation takes an average time of about 6 minutes.

162   3. The transmitted irradiance G_{moy} over the whole surface of the solar PV glass is then

163   determined by calculating the arithmetical average of the 24 G_i measured.

164   G_i and G both have been measured using a solar power meter.

165

166   *2.2. Artificial Neural Network approach*

167   Artificial Neural Networks (ANN) are artificial intelligence algorithms inspired by the

168   functioning of the nervous system. They are integrated by a number of interconnected units,

169   called neurons, that present a natural tendency to learn from the information of the outside

170   world. The main characteristic of these models is that they do not require knowledge of the

171   study phenomenon [24].

172   ANN are used to estimate functions that depend on a large number of parameters. In an

173   ANN neuron, each input parameter is assigned with an appropriate weighting factor (**W**).

174   The sum of the weighted inputs and the bias (**b**) is evaluated in a transfer function which

175   generates an output value that interacts with other neurons [25]. The architecture of ANN is

176   usually divided into three parts: an input layer, a hidden layer(s) and an output layer (Figure

177   2). To solve the non-linear multivariable phenomena, ANN are subjected to an iterative

178   process called training. This process is performed using specific algorithms, where one of

179   the most used is the Back-Propagation [22]. In the training process, the network modifies the

180   weights and bias values according to the computed error between simulated output and

181   experimental samples, a process that is repeated until obtaining a model that describes

182   accurately the studied phenomenon. The trial and error approach is the most basic method
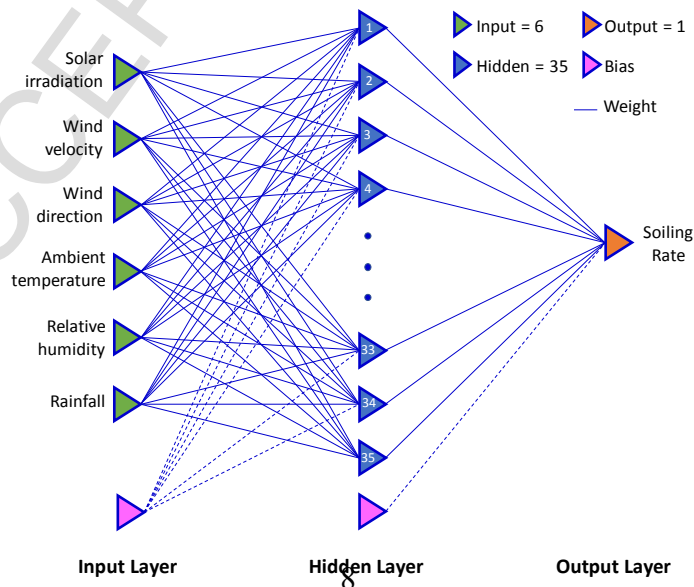
183   for training a neural network.

184

185

186

187

188

189

190

191

192

193

8

194

195

196   Figure 2. Artificial Neural Network architecture for soiling rate estimation.

197   *2.3. Mathematical modeling development*

198   An iterative numerical procedure was conducted in order to train and determine the ANN

199   model that provides the best PV glass soiling rate estimation. The implemented procedure

200   consists of three steps: (I) Creation and segmentation of the working database, (II) ANN

201   architectures design and training, and (III) statistical comparison of ANN models. A

202   graphical synthesis of the computational methodology is illustrated in Figure 3.

203   (I) A working database was formed based on the parameters recorded by the measurement

204   equipment: solar irradiance [68 W/m^2, 1182 W/m^2], wind speed [0.13 m/s, 2.74 m/s],

205   wind direction [0°, 350°], ambient temperature [11.4 °C, 31.2 °C], relative humidity [28%,

206   89%], rainfall [0 mm, 32.7 mm], and PV glass soiling rate [1.65%, 19.84%]. Table 3

207   synthesizes the presented data sets.

208

Table 3. Parameters used for the mathematical modeling process.

Parameters		Min	Max	Units
Inputs				
Solar irradiance	(G)	68	1182	[W/m²]
Wind speed	(W_s)	0.13	2.74	[m/s]
Wind direction	(W_d)	0	350	[°]
Ambient temperature	(T_{amb})	11.4	31.2	[°C]
Relative humidity	(RH)	29	89	[%]
Rainfall	(RF)	0	32.7	[mm]
Output				
PV glasses soiling rate	(SR)	1.65	19.84	[%]

209

210   Previous to the training process, the working database was normalized between 0.1 and

211   0.9 to avoid numerical overflows because of very large or small weights [26]. Database

212   normalization was given by the following equation:

213

$$x = \frac{X_i}{1.1 \times X_{max}} \tag{3}$$

214

215   where x represents the normalized value of X_i, and X_{max} is the maximum value of X_i. The

216   database was randomly divided into three segments for ANN training process: 80 % was

9

217 destined to training phase, 10 % for validation phase, and 10 % for testing. The random
218 division was used to guarantee the accurate representation of the data distribution.

219 (II) To obtain a model that provides reliable estimations of PV glass soiling rate, several
220 ANN architectures were evaluated. Figure 2 illustrates the basic ANN architecture used, it is
221 composed of 6 neurons in the input layer corresponding to solar irradiance, wind speed, wind
222 direction, ambient temperature, relative humidity, and rainfall; and one neuron in the output
223 layer given by the PV glass soling rate. The transfer functions employed for nonlinear
224 solutions are the hyperbolic tangent sigmoid (*Tansig*, Eq. 4) for the hidden layer and the
225 linear transfer function (*Purline*, Eq. 5) for the output layer [27]:

226

$$Tansig(n) = \frac{1}{1 + exp\,(- 2n)} - 1 \tag{4}$$

227

$$Purline(n) = n \tag{5}$$

228
229 where *n* represents the weighted sum of the input values. The Levenberg-Marquardt (LM)
230 backpropagation algorithm (a derivation of the Newton method) was employed to obtain the
231 optimum weights and bias values for the ANN models, due to being one of the most
232 successful algorithms in increasing the convergence speed of an ANN architectures [28].
233 Moreover, an architecture with a single hidden layer was used, because it presents a simpler
234 computation and fewer weights error propagation compared to architectures with two or
235 more hidden layers [29,30]. The progressive increment of neurons in the hidden layer was
236 the computational strategy used to find out the appropriate network architecture.

237 (III) To measure the estimation accuracy of the ANN architecture, statistical comparisons
238 between simulated outputs and experimental values were conducted. The mathematical error
239 criteria used for the comparisons were the Root Mean Square Error (RMSE) used to measure
240 the difference between the model predicted respect to the experimental measures; the Mean
241 Absolute Percentage Error (MAPE) that computes the percentage error of the model
242 numerical estimates;   and the Coefficient of Determination (R^2) determines the linear
243 relationship between experimental and simulated data between (0, 1) [31]:

244

$$RMSE = \sqrt{\dfrac{\sum\limits_{i=1}^{n}\left(SR_{Exp(i)} - SR_{Sim(i)}\right)^2}{n}} \tag{6}$$

245

$$MAPE = \dfrac{\sum\limits_{i=1}^{n}\left|\dfrac{SR_{Exp(i)} - SR_{Sim(i)}}{SR_{Exp(i)}}\right|}{n} \times 100 \tag{7}$$

246

$$R^2 = 1 - \dfrac{\sum\limits_{i=1}^{n}\left(SR_{Exp(i)} - SR_{Sim(i)}\right)^2}{\sum\limits_{i=1}^{n}\left(SR_{Exp(i)} - \overline{SR}_{Exp}\right)^2} \tag{8}$$

247
248 where $SR_{Exp(i)}$ is the measured PV glass soiling rate, $SR_{Sim(i)}$ is the simulated ANN output,

249 and $\overline{SR}_{Exp}$ is the average experimental PV glass soiling rate. As it can be appreciated in

250 Figure 3, while these statistical criteria are not satisfactory, the architecture of ANN is

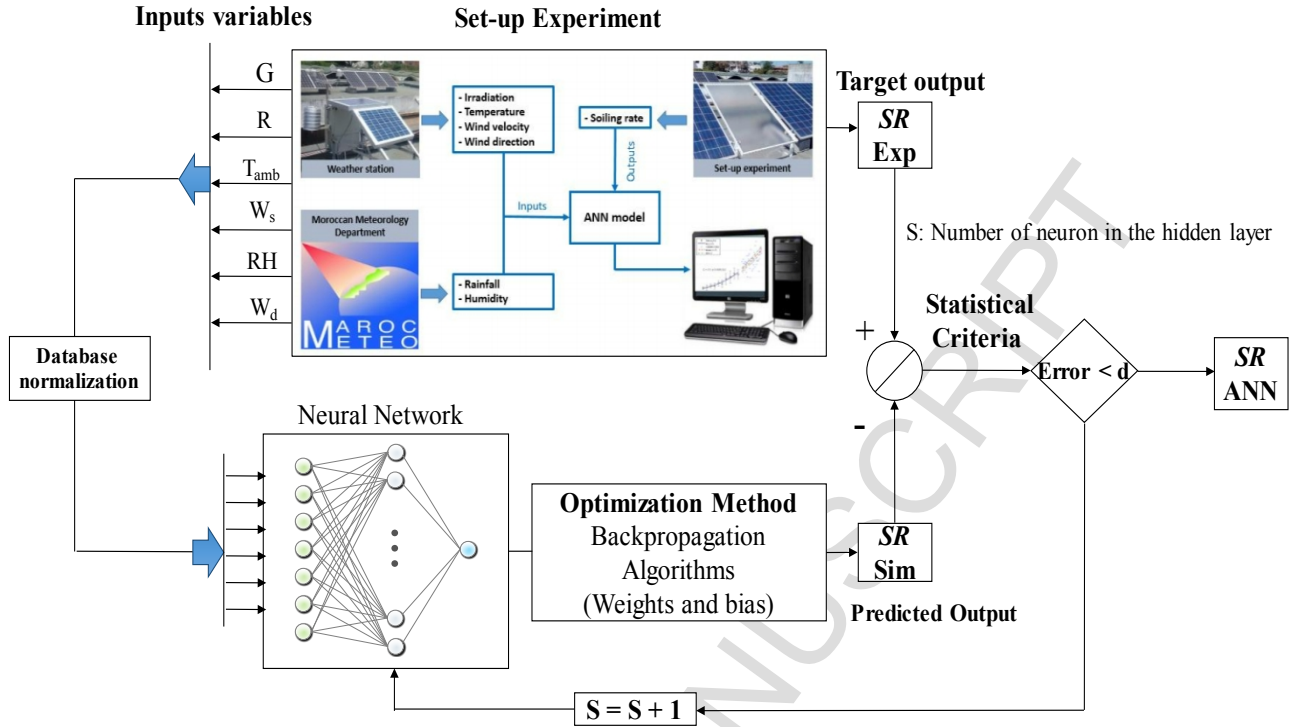251 modified and the training process is repeated.

252

11

253

254   Figure 3. The numerical procedure used for the ANN learning process, and the iterative architecture
255   used by the model to estimate soiling rate on PV modules.

256

2.4. Global Sensitivity Analysis

258   Global Sensitivity analysis (GSA) is a set mathematical techniques to understanding the
259   relative contribution of the different input parameters ($x_i = x_1, x_2...x_M$) in the output response
260   of a mathematical model (y). The use of GSA allows to identify the coherence of the model
261   with the real world and determine if the relationship is adequate.

262   In the present work, PAWN sensitivity analysis was selected due its low computational
263   cost and successful results in non-linear computational models [32]. This technique is based
264   on calculating the sensitivity to input x_i as a measure of the distance between the
265   unconditional cumulative distribution function of y ($F_y(y)$), obtained when all inputs vary
266   simultaneously, and the conditional cumulative distribution functions ($F_{y|x_i}(y)$), obtained
267   when varying all inputs with fixed x_i ($x_{\sim i}$). The Kolmogorov-Smirnov (KS) statistic is used to
268   evaluate the distance between unconditional and conditionals cumulative distribution
269   functions (CDFs):

270

$$KS = max_y \left| F_y(y) - F_{y|x_i}(y) \right| \tag{9}$$

271

272   As KS depends on the fixed value of x_i, it is calculated a PAWN sensitivity index (T_i)

273   considering a statistic over all possible values of x_i:

274

$$T_i = \overset{stat}{\underset{x_i}{}} \left[KS(x_i) \right] \tag{10}$$

275

276   A numerical approximation is required to realize this procedure, illustrated in Figure 4. As it

277   can be seen, it is divided in conditional and unconditional part. The unconditional CDF is

278   approximated by evaluating N_u random samples, for all input parameters, in the mathematical

279   model. On the other hand, to compute the conditionals CDF, g random samples are generated

280   for each input parameter ($x_i = x_1, x_2...x_M$), called conditioning values. For each conditioning

281   value, a conditional CDF is approximated using N_c output evaluations obtained keeping the

282   g value for x_i fixed and sampling random the non-fixed inputs ($x_{\sim i}$). Finally, the KS statistic

283   between unconditional and conditional CDFs is computed where KS distance indicates that

284   the x_i parameter is very influential on the model output. The total number of model

285   evaluations required to calculate the sensitivity value is $N_u + g \times N_c \times M$. The values of g,
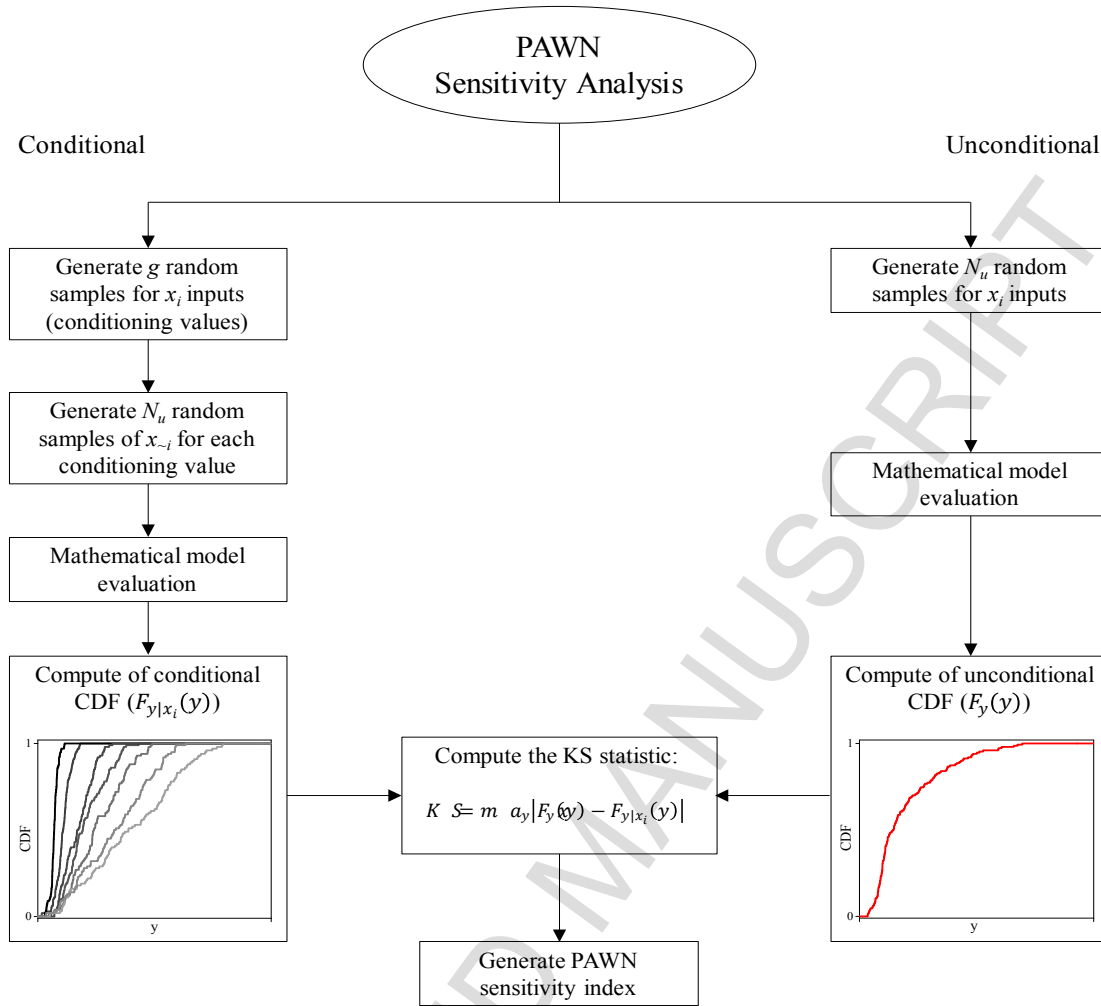
286   N_c, and N_u are chosen by trial-and-error.

13

287

288   Figure 4. Schematic diagram of computational PAWN sensitivity analysis procedure.

289

290   **3. RESULTS AND DISCUSSIONS**

291   *3.1. ANN model*

292   In order to determine the optimal ANN architecture, several network configurations were

293   trained and statistically compared (Eq. 6-8) varying the number of neurons in the hidden

294   layer from 1-35. Mathematical software MATLAB and its ANN toolbox [28] were used to

295   carry out the training process. Table 4 offers the results of the comparison between the

296   simulated data obtained from the ANN architectures and experimental PV soiling rate

297   measurements. According to Table 4, it can be noticed that the best ANN model prediction

298   was obtained with 35 neurons in the hidden layer, generating a 6-35-1 ANN architecture

299   (Figure 2). This model presents the smallest MAPE = 9.04 % and RMSE = 0.454.

14

300

Table 4. Artificial Neural Network architecture training results

ANN architecture	RMSE	MAPE	R^2	Best linear fitting
6-05-1	2.7527	32.8278	0.4727	y = 0.4633x + 4.6382
6-10-1	2.2664	25.7170	0.6271	y = 0.6252x + 3.2394
6-15-1	1.8280	19.4327	0.7579	y = 0.7558x + 2.1105
6-20-1	1.5040	13.9452	0.8346	y = 0.8346x + 1.4298
6-25-1	1.2318	10.8434	0.9051	y = 0.8224x + 0.9045
6-30-1	0.7597	9.2258	0.9175	y = 0.9075x + 0.4000
6-35-1	*0.4540*	*9.0398*	*0.9286*	*y = 0.9258x + 0.0288*

301
302

303   Figure 5 illustrates the linear regression fit between the experimental data and the results

304   of the best ANN model using all the data available (training, testing, and validation). As it

305   can be appreciated, the comparison between experimental (SR_{Exp}) and simulated (SR_{Sim})

306   obtained a satisfactory determination with a linear behavior fitting of R^2=92.8%, given by

307   linear regression model:

$$SR_{Sim} = 0.9258 \times SR_{Exp} + 0.0288 \qquad (11)$$

308

309
310
311
312
313
314
315
316
317
318
319
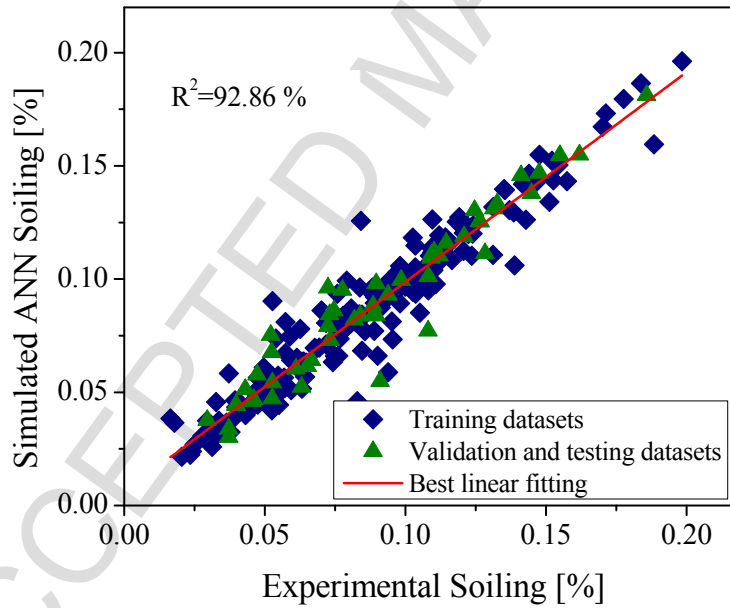
320   Figure 5. Statistical comparison between experimental soiling measurement and simulated soiling
321   result from the best ANN architecture.
322

323   Table 5 enlists the optimum weights and bias obtained for the best ANN model, where IW

324   and LW represent the input weights for the hidden layer and output layer respectively, K and

325   S are the total input (K = 6) and neuron (S = 35) numbers, and b1 and b2 the bias factor.

15

326   Based on the developed ANN architecture (Figure 2), the logarithmic sigmoid transfer

327   function (Eq. 4), the linear transfer function (Eq. 5), and the values presented in Table 5, the

328   ANN model can be analytically represented by the following equation:

329

$$SR_{Sim} = \sum_{s=1}^{S} \left[LW(1,s) \left(\frac{1}{1 + \exp\left(-2\left(\sum_{k=1}^{K} (IW(s,k)\, x(k)) + b_1(s)\right)\right)} \right) + 1 \right] + b_2 \quad (12)$$

330

331   where x is the parameter value corresponding operation and LW, IW, b1, b2, K, and S are

332   described in Table 5.

333

334   Table 5. Weights and bias parameters obtained for the ANN model developed.

Hidden neurons (s)	Weights						Output layer LW(s,l)	Bias	
	Hidden layer (S=35, K=6) IW (s,k)								
	G (k=1)	W_s (k=2)	W_d(k=3)	T_{amb}(k=4)	RH (k=5)	RF (k=6)	SR (%)	b1	b2
1	-4.788	-0.289	-3.069	6.017	-1.715	-5.651	-14.478	-4.961	-1.930
2	1.800	-1.903	17.128	-1.227	-1.249	7.849	3.141	25.201	
3	-2.787	-0.861	-0.515	0.130	0.714	-3.057	14.848	-0.076	
4	-3.695	4.278	-0.741	2.866	5.506	4.479	-13.730	3.071	
5	-3.648	4.898	10.007	21.894	1.109	-5.269	-1.752	2.916	
6	0.913	2.801	6.207	0.125	-0.744	3.384	19.992	13.383	
7	5.879	3.290	7.435	7.199	3.376	3.441	7.910	0.820	
8	3.059	-5.496	2.105	-5.729	-2.937	15.189	-1.431	13.340	
9	4.908	0.545	4.856	-6.214	1.994	5.417	-12.475	6.272	
10	10.413	19.911	-6.890	-2.676	16.361	-7.085	0.693	-8.692	
11	-3.281	4.025	-0.186	2.688	4.820	4.645	15.518	3.960	
12	-13.070	-4.373	17.345	-15.929	-5.364	-5.184	-1.756	1.421	
13	5.920	-0.007	-8.455	-5.127	-6.689	6.924	6.312	-8.187	
14	-22.619	-4.441	8.296	13.944	-0.190	0.835	-0.468	11.735	
15	-2.749	-4.286	-2.032	-1.285	-1.173	0.002	-10.818	-0.686	
16	-9.973	-4.816	1.721	-44.492	-3.166	-2.532	0.571	11.219	
17	-11.632	-26.119	48.205	-23.840	-27.839	-4.195	-0.730	26.050	
18	6.304	-6.812	-10.102	6.815	-5.481	17.343	6.252	-4.118	
19	5.782	-2.033	6.166	-0.691	-1.799	12.291	5.382	6.947	
20	-37.417	12.972	-8.495	15.609	13.660	-16.278	-0.290	3.964	
21	-0.963	2.922	4.249	12.460	2.079	-5.783	3.087	-3.579	
22	-31.520	-17.327	-5.951	13.010	-7.637	-6.037	0.549	-6.039	
23	3.463	3.029	-5.686	0.088	3.747	6.629	1.679	7.869	
24	-12.464	-1.498	-3.459	-0.294	-4.565	2.364	4.955	-3.106	
25	-2.126	3.502	5.986	-3.452	2.703	-6.267	8.269	5.119	
26	-0.002	1.239	11.584	1.478	2.468	4.344	-2.512	14.643	
27	-9.983	2.081	-18.152	-4.788	6.500	-7.357	-1.035	-19.017	

28	-2.889	-3.748	-2.116	-1.278	-1.692	0.155	15.920	-0.064
29	7.806	7.447	-0.222	-5.315	2.029	21.265	3.664	22.659
30	2.205	2.057	0.332	0.313	2.199	-0.063	7.532	-1.882
31	-0.494	-2.504	2.061	-0.282	-0.288	0.027	5.037	0.464
32	5.828	-0.531	-15.515	-7.052	0.701	8.594	-1.983	-10.011
33	-9.450	-7.380	-0.533	6.303	-1.810	-23.295	3.149	-25.229
34	17.699	2.093	8.771	-1.912	2.641	-6.171	3.342	7.265
35	2.413	5.784	-0.052	10.588	1.246	2.347	-16.369	16.283

335

336   *3.2. Sensitivity analysis results*

337   Sensitivity analysis was carried out using the computational package SAFE 1.1 [33]. The

338   assigned N_u, N_c, and g values were 1200, 900, and 45 respectively, obtained by an iterative

339   evaluation procedure. The N_u and N_c random samples were generated considering the

340   minimum and maximum values of each parameter (Table 3). Figure 6 illustrates the

341   unconditional and conditional CDFs output response of the PV glass soiling rate model

342   developed. The red lines represent the unconditional CDFs ($F_y(y)$), and the gray-scale lines

343   are the conditional CDFs ($F_{y|x_i}(y)$) at different fixed values of the analyzed parameter (x_i).

344   As it can be seen in Figure 6, the $F_{y|x_i}(y)$ curves of input parameters present different

345   cumulative densities distanced of their respective $F_y(y)$. This behavior indicates the effect

346   of x_i on the PV glass soiling rate predicted. In the case of relative humidity, wind direction,

347   and wind speed, a greater separation distance between $F_{y|x_i}(y)$ and $F_y(y)$ curves are

348   observed. This indicates that these parameters have a significant effect on the model

349   response. On the contrary, for rainfall and ambient temperature, the curves $F_{y|x_i}(y)$

350   approximate to $F_y(y)$ determining that both parameters have less influence on the model

351   output.

352   Figure 6 also provides information about the model behavior when modifying the value

353   of the fixed input parameter from lowest (dark $F_{y|x_i}(y)$ lines) to greater (clear $F_{y|x_i}(y)$ lines).

354   It can be observed in Figure 6(a), that increments in the solar irradiance values decrease the

355   model output response, while higher dust deposition occurs in the presence of low radiation.

356   Similar case is presented in Figure 6(b), where according to the model the soiling deposition

357   is favored by the low wind velocities, which is consistent with the physical behavior of the

358   phenomenon. On the other hand, from Figure 6(c) and 6(e), it is observed that the soling rate

17

359 is directly proportional to variations of wind direction and relative humidity. Finally, for

360 ambient temperature and rainfall (Figure 6(d) and 6(f)) it is not possible to make a clear

361 description due to the low sensitivity they present.

362   A sensitivity index (T_i) is calculated considering a statistic over all possible values of x_i in

363 order to synthesize the cumulative density distribution curves analysis results. The T_i

364 provides a value that describes the model sensitivity respect to the variable. Table 6 shows

365 the summarizes sensitivity analysis information. T_i results indicate that relative humidity was

366 the most significant parameter (0.2122) for PV soiling deposition following by wind

367 direction (0.2103), wind speed (0.1778), solar radiation (0.1733), ambient temperature

368 (0.1689), and rainfall (0.1458). It is important to indicate that the indexes of the parameters

369 are close to each other. It determines that although the influence of some is smaller their

370 contribution is important for the modeling process.

371

372

373

Table 6. Relative importance of input variables.

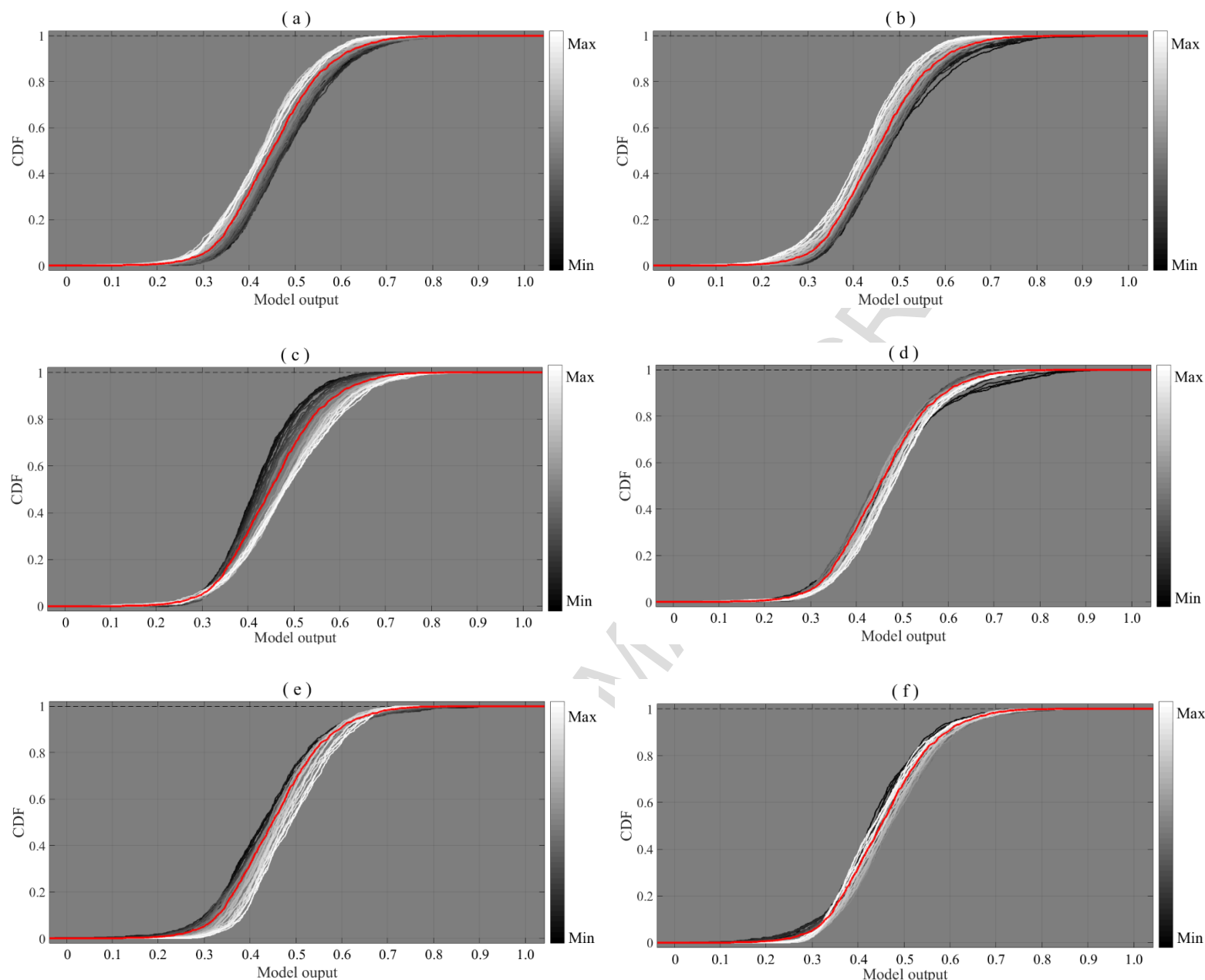| Parameter	Sensitivity Index
Solar irradiance	0.1733
Wind speed	0.1778
Wind direction	0.2103
Ambient temperature	0.1689
Relative humidity	0.2122
Rainfall	0.1458

374

Figure 6. Cumulative density distribution curves of the model output for each input parameters. (a) solar irradiance, (b) wind speed, (c) wind direction, (d) ambient temperature, (e) relative humidity, (f) rainfall.

19

4. CONCLUSIONS

This paper proposed a computational methodology for estimation of soiling rate on solar PV panels. An Artificial Neural Network (ANN) model was developed to express the soiling rate in function of the environmental parameters solar irradiance, wind speed, wind direction, ambient temperature, relative humidity, and rainfall. The model was trained with experimental data from Moroccan Meteorology Department and Solar Energy Platform in Rabat, Morocco. The performance of the model was statistically evaluated and compared with information not used in the modeling process. The statistical results indicate that the ANN model has an adequate estimation capacity for the given conditions of the case study.

In addition, a new sensitivity analysis technique is employed to determine the effects of input parameters in the response of the ANN model. The sensitivity analysis results indicate that all the parameters have a relevant contribution on model output, begging the most influential the relative humidity followed by wind direction, wind speed, solar irradiance, ambient temperature, and rainfall. Sensitivity analysis also showed the behavior of the model output for variation of each input parameter in a wide range value (from maximum to minimum). This provides a more detailed description of the model allowing to visualize its ability to adapt to the phenomenon of study.

This work lays the foundation for modeling based on more detailed artificial intelligence techniques that consider greater geographic extensions, different annual conditions and longer periods of measurement. On the other hand, it was also demonstrated that the employed sensitivity analysis proves to be a powerful tool that allows describing the physics of the phenomenon from the ANN model.

This kind of analysis can be implemented in other renewable energy model based on artificial intelligence to complete the empty knowledge that leaves the use of these techniques in the physical understanding of the phenomenon. Finally, this method is a promising framework for its application in smart sensors on cleaning systems for PV modules to improve their operational efficiency.

419

420 REFERENCES

421 [1]   OECD, Public-Private Partnerships in the Middle East and North Africa. A Handbook for Policy
422   Makers, (2014) 121.

423 [2]   S. Bouaddi, A. Ihlal, A. Fernández-García, Soiled CSP solar reflectors modeling using dynamic linear
424   models, Sol. Energy. 122 (2015) 847–863. doi:10.1016/j.solener.2015.09.044.

425 [3]   M. Karim, S. Naamane, C. Delord, Evaluation of the behaviour of different solar mirrors against soiling
426   phenomenon, in: 2016 Int. Renew. Sustain. Energy Conf., IEEE, 2016: pp. 326–329.
427   doi:10.1109/IRSEC.2016.7984008.

428 [4]   A.A. Merrouni, F. Wolfertstetter, A. Mezrhab, S. Wilbert, R. Pitz-Paal, Investigation of Soiling Effect
429   on Different Solar Mirror Materials under Moroccan Climate, Energy Procedia. 69 (2015) 1948–1957.
430   doi:10.1016/j.egypro.2015.03.194.

431 [5]   C. Schill, S. Brachmann, M. Koehl, Impact of soiling on IV-curves and efficiency of PV-modules, Sol.
432   Energy. 112 (2015). doi:10.1016/j.solener.2014.12.003.

433 [6]   P. Sinha, W. Hayes, B. Littmann, L. Ngan, R. Znaidi, Environmental variables affecting solar
434   photovoltaic energy generation in Morocco, in: 2014 Int. Renew. Sustain. Energy Conf., IEEE, 2014:
435   pp. 230–234. doi:10.1109/IRSEC.2014.7059897.

436 [7]   W. Anana, F. Chaouki, B. Laarabi, D. Dahlioui, M.A. Sebbar, A. Barhdadi, V. Gilioli, D. Verdilio,
437   Soiling impact on energy generation of high concentration Photovoltaic power plant in Morocco, in:
438   2016 Int. Renew. Sustain. Energy Conf., IEEE, 2016: pp. 234–238. doi:10.1109/IRSEC.2016.7983994.

439 [8]   D. Dahlioui, B. Laarabi, M.A. Sebbar, A. Barhdadi, G. Dambrine, E. Menard, J. Boardman, Soiling
440   effect on photovoltaic modules performance: New experimental results, in: 2016 Int. Renew. Sustain.
441   Energy Conf., IEEE, 2016: pp. 111–114. doi:10.1109/IRSEC.2016.7983955.

442 [9]   S. Bouaddi, A. Ihlal, A. Fernández-García, Comparative analysis of soiling of CSP mirror materials in
443   arid zones, Renew. Energy. 101 (2017) 437–449. doi:10.1016/j.renene.2016.08.067.

444 [10]   D.C. Miller, S.R. Kurtz, Durability of Fresnel lenses: A review specific to the concentrating
445   photovoltaic application, Sol. Energy Mater. Sol. Cells. 95 (2011) 2037–2068.
446   doi:10.1016/j.solmat.2011.01.031.

447 [11]   T. Sarver, A. Al-Qaraghuli, L.L. Kazmerski, A comprehensive review of the impact of dust on the use

448   of solar energy: History, investigations, results, literature, and mitigation approaches, Renew. Sustain.
449   Energy Rev. 22 (2013) 698–733. doi:10.1016/j.rser.2012.12.065.

450   [12]   H.K. Elminir, A.E. Ghitas, R.H. Hamid, F. El-Hussainy, M.M. Beheary, K.M. Abdel-Moneim, Effect
451   of dust on the transparent cover of solar collectors, Energy Convers. Manag. 47 (2006) 3192–3203.
452   doi:10.1016/j.enconman.2006.02.014.

453   [13]   M.S. El-Shobokshy, F.M. Hussein, Effect of dust with different physical properties on the performance
454   of photovoltaic cells, Sol. Energy. 51 (1993) 505–511. doi:10.1016/0038-092X(93)90135-B.

455   [14]   H. Khonkar, A. Alyahya, M. Aljuwaied, M. Halawani, A. Al Saferan, F. Al-khaldi, F. Alhadlaq, B.A.
456   Wacaser, Importance of cleaning concentrated photovoltaic arrays in a desert environment, Sol. Energy.
457   110 (2014) 268–275. doi:10.1016/j.solener.2014.08.001.

458   [15]   J. Yun, L. Verma, A. James, H. Yang, The Effect of Dust on Transmission and Self-cleaning Property
459   of Solar Panels, 15 (2012) 421–427. doi:10.1016/j.egypro.2012.02.051.

460   [16]   A. Sayyah, M.N. Horenstein, M.K. Mazumder, Energy yield loss caused by dust deposition on
461   photovoltaic panels, Sol. Energy. 107 (2014) 576–604. doi:10.1016/j.solener.2014.05.030.

462   [17]   R. De Leone, M. Pietrini, A. Giovannelli, Photovoltaic energy production forecast using support vector
463   regression, Neural Comput. Appl. 26 (2015) 1955–1962. doi:10.1007/s00521-015-1842-y.

464   [18]   R.V.A. Monteiro, G.C. Guimarães, F.A.M. Moura, M.R.M.C. Albertini, M.K. Albertini, Estimating
465   photovoltaic power generation: Performance analysis of artificial neural networks, Support Vector
466   Machine   and   Kalman   filter,   Electr.   Power   Syst.   Res.   143   (2016)   643–656.
467   doi:10.1016/j.epsr.2016.10.050.

468   [19]   J. Tziu Dzib, E.J. Alejos Moo, A. Bassam, M. Flota-Bañuelos, M.A. Escalante Soberanis, L.J. Ricalde,
469   M.J. López-Sánchez, Photovoltaic Module Temperature Estimation: A Comparison Between Artificial
470   Neural Networks and Adaptive Neuro Fuzzy Inference Systems Models, in: Intell. Comput. Syst., 2016:
471   pp. 46–60. doi:10.1007/978-3-319-30447-2.

472   [20]   A. Bassam, O. May Tzuc, M.A. Escalante Soberanis, L.J. Ricalde, B. Cruz, Temperature Estimation
473   for Photovoltaic Array Using an Adaptive Neuro Fuzzy Inference System, Sustainability. 9 (2017)
474   1399. doi:10.3390/su9081399.

475   [21]   A.A.A. Darwish, T.A. Hanafy, A.A. Attia, D.M. Habashy, M.Y. El-Bakry, M.M. El-Nahass,
476   Optoelectronic performance and artificial neural networks (ANNs) modeling of n-InSe/p-Si solar cell,
477   Superlattices Microstruct. 83 (2015) 299–309. doi:10.1016/j.spmi.2015.03.033.

478   [22]   M. Kamran, S.A. Haider, T. Akram, S.R. Naqvi, S.K. He, Prediction of IV curves for a superconducting
479   thin   film   using   artificial   neural   networks,   Superlattices   Microstruct.   95   (2016)   88–94.
480   doi:10.1016/j.spmi.2016.04.018.

481   [23]   R.K. Kharb, S.L. Shimi, S. Chatterji, M.F. Ansari, Modeling of solar PV module and maximum power
482   point   tracking   using   ANFIS,   Renew.   Sustain.   Energy   Rev.   33   (2014)   602–612.
483   doi:10.1016/j.rser.2014.02.014.

484   [24]   S. Haykin, Neural networks, Upper Saddle River, NJ Prentice Hall., 1999.

485   [25]   A. Espinosa Guzmán, O. May Tzuc, I. Balam Pantí, J. Reyes Trujeque, I. Pérez Quintana, A. Bassam,

486   Modelado de partículas PM10 y PM2.5 Mediante Redes Neuronales Artificiales sobre clima tropical
487   de San Francisco de Campeche, México, Quim. Nova. In Press (2017) 1–10. doi:10.21577/0100-
488   4042.20170115.

489 [26] A.M. Ghaedi, M. Ghaedi, A.R. Pouranfard, A. Ansari, Z. Avazzadeh, A. Vafaei, I. Tyagi, S. Agarwal,
490   V.K. Gupta, Adsorption of Triamterene on multi-walled and single-walled carbon nanotubes: Artificial
491   neural network modeling and genetic algorithm optimization, J. Mol. Liq. 216 (2016) 654–665.
492   doi:10.1016/j.molliq.2016.01.068.

493 [27] O. May Tzuc, A. Bassam, M.A. Escalante Soberanis, E. Venegas-Reyes, O.A. Jaramillo, L.J. Ricalde,
494   E.E. Ordoñez, Y. El Hamzaoui, Modeling and optimization of a solar parabolic trough concentrator
495   system using inverse artificial neural network, J. Renew. Sustain. Energy. 9 (2017) 13701.
496   doi:10.1063/1.4974778.

497 [28] M.H. Beale, M.T. Hagan, H.B. Demuth, Neural Network Toolbox™ User's Guide R2017a, The
498   MathWorks, Inc., 2017.

499 [29] J. de Villiers, E. Barnard, Backpropagation Neural Nets with One and Two Hidden Layers, IEEE Trans.
500   Neural Networks. 4 (1993) 136–141. doi:10.1109/72.182704.

501 [30] S.K. Biswas, M. Chakraborty, H.R. Singh, D. Devi, B. Purkayastha, A.K. Das, Hybrid case-based
502   reasoning system by cost-sensitive neural network for classification, Soft Comput. (2016) 1–18.
503   doi:10.1007/s00500-016-2312-x.

504 [31] Y. El Hamzaoui, M. Abatal, A. Bassam, F. Anguebes-Franseschi, O. Oubram, I. Castaneda Robles, O.
505   May Tzuc, Artificial neural networks for modeling and optimization of phenol and nitrophenols
506   adsorption onto natural activated carbon, Desalin. Water Treat. 58 (2017) 2002–213.
507   doi:10.5004/dwt.2017.1705.

508 [32] F. Pianosi, T. Wagener, A simple and efficient method for global sensitivity analysis based on
509   cumulative distribution functions, Environ. Model. Softw. 67 (2015) 1–11.
510   doi:10.1016/j.envsoft.2015.01.004.

511 [33] F. Pianosi, F. Sarrazin, T. Wagener, A Matlab toolbox for Global Sensitivity Analysis, Environ. Model.
512   Softw. 70 (2015) 80–85. doi:10.1016/j.envsoft.2015.04.009.

513

Highlights

- An artificial neural network methodology has been proposed for modeling soiling rate on solar photovoltaic glass.

- Artificial neural network was trained and testing using environmental variables.

- Statistical criteria were employed to measure the error between experimental and the predicted results.

- A sensitivity analysis approach was employed to determine the effect of input parameter on model output.